

W L_{III} -edge XANES and EXAFS studies of $Pb(Fe_{2/3}W_{1/3})O_3$ - $PbTiO_3$ multiferroic ceramics

This content has been downloaded from IOPscience. Please scroll down to see the full text.

2013 J. Phys.: Conf. Ser. 430 012111

(<http://iopscience.iop.org/1742-6596/430/1/012111>)

View [the table of contents for this issue](#), or go to the [journal homepage](#) for more

Download details:

IP Address: 200.133.225.27

This content was downloaded on 21/03/2017 at 18:14

Please note that [terms and conditions apply](#).

You may also be interested in:

[Tracking the Formation of Nano-sized Zinc Oxide from Zinc Peroxide by In Situ XAS and XRD](#)

T Daley, E Raj, S Ramos et al.

[EXAFS study of PZT ferroelectric thin films of different crystallinities](#)

X P Hu, D W Duan, K Zhang et al.

[Order-disorder nature of the antiferroelectric transition in \$Pb_2MnWO_6\$](#)

G Subías, J Blasco, J García et al.

[XANES Study of the Radiation Damage on Alkanethiolates-Capped Au Nanoparticles](#)

J M Ramallo-López, L J Giovanetti, F C Vicentin et al.

[A new metal exchanged zeolite for a present environmental problem. An in-situ XAS study](#)

C Alonso-Escobar, C Franch-Martí, A E Palomares et al.

[An in-situ heater for the XAS beamline \(12-ID\) in Australia](#)

B Johannessen, Z S Hussain, D R East et al.

W L_{III} -edge XANES and EXAFS studies of $Pb(Fe_{2/3}W_{1/3})O_3$ - $PbTiO_3$ multiferroic ceramics

Alexandre Mesquita¹, Bárbara Maraston Fraygola¹, Valmor Roberto Mastelaro² and José Antonio Eiras¹

¹Departamento de Física, Universidade Federal de São Carlos, São Carlos, SP, Brazil

²Instituto de Física de São Carlos, Universidade de São Paulo, São Carlos, SP, Brazil

E-mail: valmor@ifsc.usp.br

Abstract. The local structure of $Pb(Fe_{2/3}W_{1/3})O_3$ (PFW) and $Pb(Fe_{2/3}W_{1/3})O_3$ - $PbTiO_3$ (PFW100xPT, $x=0.10$ and $x=0.20$) multiferroic ceramics was probed by X-ray absorption spectroscopy at the W L_{III} -edge. The analysis of XANES spectra did not show significant modifications in the intensity or energy of transitions as a function of temperature or $PbTiO_3$ content. The fitting of EXAFS spectra of PFW samples revealed a local rhombohedral symmetry of W atoms around 120 K, which is consistent with the electrical properties of this compound. Concerning the local structure of W atoms in PFW100xPT samples, in all cases, at 290 K, a local tetragonal symmetry was determined although by X-ray diffraction a cubic local symmetry was expected.

1. Introduction

Multiferroic materials have attracted the attention of many researchers in the last years due the coexistence of magnetic and electric ordering [1]. The research with these materials is driven by the prospect of controlling charges by applied magnetic fields or spins by applied voltages, and using this ability to construct new forms of multifunctional devices [1]. The magnetoelectric coupling can be observed in multiferroic materials in the regions where magnetic and ferroelectric ordering coexists and in many cases, is mediate via lattice strain [2].

Among these materials, lead iron tungstate $Pb(Fe_{2/3}W_{1/3})O_3$ (PFW) is known as a perovskite-type structure in which Fe^{3+} and W^{6+} are randomly distributed at the octahedral B-site positions and presents ferroelectric and antiferromagnetic ordering. PFW has a frequency dependent permittivity with a broad maximum around 180 K which makes difficult practical applications [2]. Challenges for technological applications require preferentially that the magnetic and ferroelectric ordering coexistence occurs around room temperature and a low electric conductivity, in order to enable the poling of the sample. Thus, the addition of $PbTiO_3$ to PFW structure, forming the $(1-x)Pb(Fe_{2/3}W_{1/3})O_3$ - $xPbTiO_3$ (PFW-PT) system causes symmetry changes and on the range of temperature where magnetic and ferroelectric ordering coexists, depending on the $PbTiO_3$ contents [3]. Moreover, a transition from relaxor to normal ferroelectric state is induced as the $PbTiO_3$ content increases [2].

Although the long-range structure and the electrical/magnetic properties of these compounds has been characterized in order to better understand the processes of phase transition and electrical/magnetic behaviour of these compounds, as far as authors know, there are no available studies concerning the local structure of PFW-PT compounds probed by X-ray absorption spectroscopy (XAS). Thus, the present paper concerns a study about the local order and electronic

structure of PFW and PFW-PT compounds by measuring the W L_{III} -edge EXAFS (extended X-ray absorption fine structure) and XANES (X-ray absorption near edge structure) spectra.

2. Experimental

The two-stage solid-state reaction process first used by Swartz and ShROUT to synthesize the perovskite $Pb(Mn_{2/3}Nb_{1/3})O_3$ PMN compound, was used in this study to prepare PFW and PFW-PT samples and experimental details about samples preparation are given elsewhere [2,4]. Ceramic samples of $(1-x)Pb(Fe_{2/3}W_{1/3})O_3-xPbTiO_3$ (PFW100xPT) compositions were prepared with $x = 0.00, 0.10$ and 0.20 .

EXAFS and XANES spectra at the W L_{III} -edge were collected in transmission mode as a function of the temperature (PFW samples) and sample composition (PFW100xPT samples) using a Si(111) double-crystal monochromator on the D04B-XAS2 beamline at the LNLS (National Synchrotron Light Laboratory) facility, Brazil. EXAFS spectra at the W L_{III} -edge were recorded for each sample between 10100 and 11000 eV using an energy step of 2 eV whereas XANES spectra were recorded between 10130 and 10300 eV with a energy step of 0.3 eV. The extraction and analysis of XANES and EXAFS spectra were performed using the Multi-Platform Applications for X-Ray absorption (MAX) software package [5] whereas theoretical spectra were calculated using FEFF8.2 code [6].

3. Results and discussion

Figure 1 (a) presents the XANES spectra at W L_{III} -edge of PFW sample measured at 120, 224 and 297 K and Figure 1 (b) shows the XANES spectra at W L_{III} -edge of PFW-PT samples as a function of PT content measured at 297 K. The W L_{III} -edge white line mostly derives from electron transitions from the $2p_{3/2}$ state to a vacant $5d$ state [7]. Figure 1 shows that L_{III} absorption edge presents a clear double peak structure with slightly less intensity of the peak situated at highest energy, which is identified as the signature of the crystal field splitting of the $5d$ band into t_{2g} and e_g states in a octahedral symmetry [7]. As can be seen in Figure 1 (a) and (b), no changes are observed on the XANES spectra of PFW and PFW-PT samples with the increasing of temperature or the PT content.

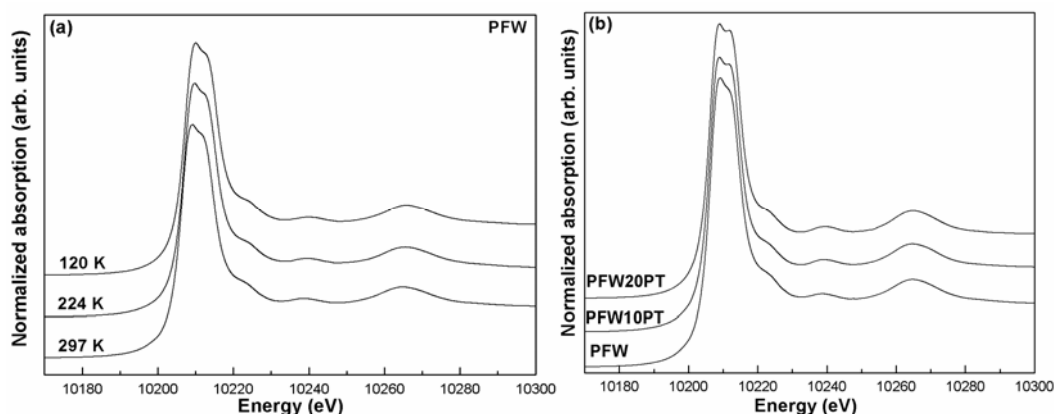


Figure 1. XANES spectra at W L_{III} -edge (a) PFW sample measured at different temperatures and (b) PFW-PT samples measured at 297 K.

In order to identify which atoms or interactions have a more significant contribution on the features observed in the W L_{III} -edge XANES spectra, theoretical spectra were calculated using CRYSTALFFREV (from MAX software package) and FEFF8.2 programs [5, 6] using the crystallographic data of PFW sample obtained from X-ray diffraction pattern collected at 297 K [8]. Figure 2 shows the calculated spectra as a function of the cluster radius around the absorber atom. The cluster radius of 6.0 Å concerns a neighbourhood around W atoms formed by 84 atoms, whereas the cluster radius of 1.98 Å concerns only the first shell of O atoms belonging to the WO_6 octahedra (6 atoms), the cluster radius of 3.45 Å includes up to the first shell of Pb atoms (14 atoms), the cluster

radius of 3.98 Å includes up to the first shell of W/Fe atoms (20 atoms) and the cluster radius of 4.45 Å includes up to the second shell of O atoms (44 atoms).

As shown in Figure 2, the spectrum calculated with a cluster radius of 6 Å reproduces quite well the white line of XANES structure and the features up to 60 eV above the edge observed in the XANES experimental spectrum of PFW sample. In the spectrum calculated with a cluster radius of 1.98 Å, it is not observed the transitions located between the edge and 10240 eV, indicating that these transitions would be originated from W-Pb interactions.

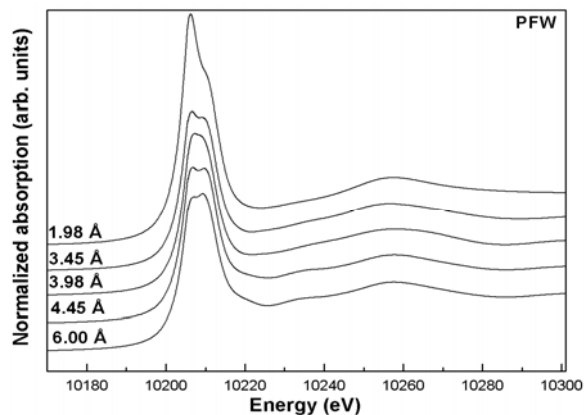


Figure 2. Theoretical XANES spectra at W L_{III} -edge of PFW sample as a function of the cluster radius.

Figure 3 (a) shows the modulus of Fourier transform of PFW sample extracted from W L_{III} -edge EXAFS spectra collected at different temperatures and Figure 3 (b) shows the modulus of Fourier transform of PFW, PFW10PT and PFW20PT samples collected at 297 K.

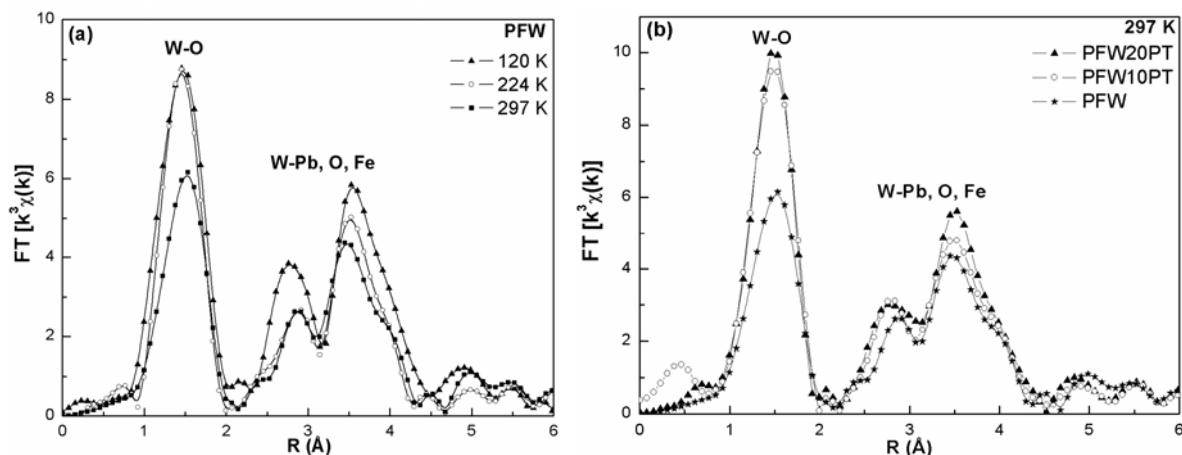


Figure 3. Modulus of Fourier transform of $k^3\chi(k)$ EXAFS spectra (a) PFW sample collected at different temperatures and (b) PFW-PT measured at 297 K.

In order to obtain qualitative structural information from EXAFS spectra, theoretical EXAFS spectra were calculated considering the reported crystalline structure of PFW sample [9]. In a study of PFW compound using neutron diffraction measurements between 10 and 700 K, Ivanov *et al.* showed that the symmetry of PFW remains cubic with a $Pm-3m$ space group. Mitoseriu *et al.* also identify a cubic symmetry for PFW at 85 K, but reported a possible separation of diffraction peaks due to a rhombohedral phase with $R3m$ space group [8]. However, these authors argue that the difference between these two types of symmetries, cubic and rhombohedral, could not be clearly detected by X-ray diffraction measurements due to the experimental accuracy [8]. Thus, theoretical EXAFS spectra

were calculated using FEFF8.2 code [6] considering structural models with a cubic ($Pm-3m$ space group), rhombohedral ($R3m$ space group) and tetragonal ($P4mm$ space group) [8] symmetries.

According to these structural models, the more intense peak, between 1.0 and 2.0 Å in the Fourier transforms of PFW sample, corresponds to a single scattering interaction between the first six O atoms and the W atoms. The single scattering interactions relative to W-Pb, W-W/Fe and W-O (beyond the first neighbours at WO_6) paths correspond the peaks and shoulders observed between 2.0 and 5.0 Å. This region also includes multiple scattering paths such as W-O-O, W-O-Fe-O, W-Pb-O, W-W-O, W-Fe-O, W-O-W-O, and W-O-O-O interactions.

As can be seen in Figure 3 (a), the position and shape of the peaks do not show significant modifications, indicating that the neighbourhood of W atom does not modify drastically with the temperature. Only the intensity of the peaks in Fourier transform, mainly the intensity relative to first peak, decreases with increasing of the temperature which occurs due to an increasing of the Debye-Waller factor since, according XRD, modifications in the neighbour number are not expected in this range of temperature. In Figure 3 (b), only an intensity increasing on the first peak of Fourier transform is observed as the amount of $PbTiO_3$ increases. This increasing can be associated with the increasing of the temperature of the ferroelectric-paraelectric phase transition [4]. For PFW sample, the temperature of ferroelectric-paraelectric phase transition is around 180 K and thus, the EXAFS spectra collected at 297 K corresponds to a cubic paraelectric phase whereas the temperature of ferroelectric-paraelectric phase transition of PFW20PT sample is around 256 K [4, 8].

In order to obtain quantitative structural results regarding the first W-O coordination shell, the first peak of the Fourier transform curves of PFW and PFW-PT samples (Figure 3) were back Fourier transformed. The experimental and theoretical EXAFS spectra concerning only the first coordination shell are shown on Figure 4. As can be seen on Figure 4(a), the best fit was those using a rhombohedral symmetry at 120 K and a cubic symmetry at 224 K and 297 K. Table I shows the interatomic distance (R), Debye-Waller factor (σ^2) and the quality factor (QF) obtained with the fitting. The fitting results on Table I show that the quality factor of the fit considering a local rhombohedral symmetry for PFW sample measured at 120 K presents a better agreement with experimental data than considering a local cubic symmetry. In the rhombohedral local symmetry, the WO_6 octahedra are formed by three different shells of two O atoms. As the temperature increases above 220 K, the best fit was performed using a local cubic symmetry model, which is in agreement with previous studies [2, 8].

The observation of a local rhombohedral symmetry for W atoms in PFW samples measured at 120 K is in apparent disagreement with previous studies which reported a cubic symmetry for PFW samples from 10 and 700 K [8, 9]. The apparent discrepancy between the XAS and neutron results can be explained in terms of the level of disorder that these techniques can detect [10,11]. As a result, XAS technique allows a better image of the local distortions because, if the symmetry were completely cubic, the structure would correspond to the paraelectric phase instead of a ferroelectric one and therefore, the observation of the ferroelectric hysteresis loops would not be expected. However, our previous study concerning electrical properties of this compound showed ferroelectric hysteresis loops at 80, 100, 160 and 200 K [4].

As illustrated in Figure 4b and Table I, the best fitting of the EXAFS spectra of PFW10PT and PFW20PT samples measured at 297 K gives a local tetragonal symmetry for the first W-O shell formed by two short WO_I and four longer WO_{II} interactions. However, at 297 K, a local cubic symmetry was expected since this temperature is respectively 65 K and 41 K higher than the temperature of the maximum of the dielectric permittivity of PFW10PT and PFW20PT samples which corresponds to the ferroelectric to paraelectric dielectric transition [4].

Thus, EXAFS results of PFW10PT and PFW20PT showed that the local structure around W atoms in these two samples remained tetragonal well above the maximum of their dielectric permittivity curves where the samples were characterized as paraelectric and presenting a cubic long-range order phase according XRD experiments [4]. These findings are similar to those observed in others lead ferroelectric ceramic materials systems [10,11]

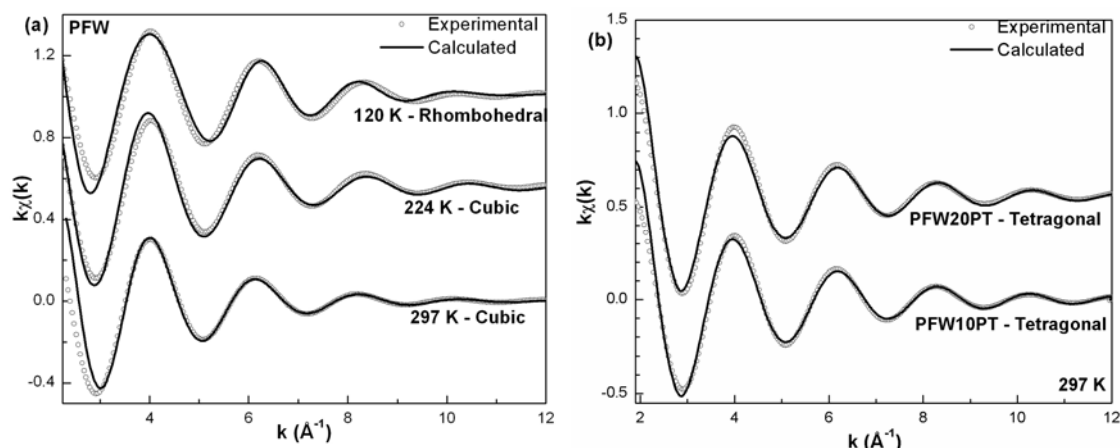


Figure 4. Fitting and back-Fourier-filtered experimental signal of the W-O first shells for (a) PFW sample at 120 K, 224 K and 297 K and (b) PFW-PT samples at room temperature.

Table I – W L_{III} -edge EXAFS fitting structural parameters of PFW as a function of the temperatures and PFW-PT samples as a function of the composition. Different structural models with rhombohedral, tetragonal and cubic symmetries were used during the fitting procedure.

Sample	Temperature	Symmetry	Shell	N	R (Å)	σ^2 (Å ²)	QF
PFW	120 K	Cubic	W-O _I	6	1.86(1)	0.0157(7)	21.71
			W -O _I	2	1.88(2)		
PFW	120 K	Rhombohedral	W -O _{II}	2	1.87(2)	0.0085(6)	5.96
			W -O _{III}	2	2.29(1)		
PFW	224 K	Cubic	W -O _I	6	1.85(1)	0.0069(11)	0.50
PFW	297 K	Cubic	W -O _I	6	1.89(1)	0.0107(7)	1.31
PFW10PT	297 K	Tetragonal	W -O _I	2	1.77(1)	0.0027(6)	0.61
			W -O _{II}	4	1.90(1)		
PFW20PT	297 K	Tetragonal	W -O _I	2	1.78(2)	0.0010(12)	0.56
			W -O _{II}	4	1.90(1)		

4. Conclusions

The local structure of $\text{Pb}(\text{Fe}_{2/3}\text{W}_{1/3})\text{O}_3\text{-PbTiO}_3$ multiferroic ceramics was probed by XAS at W L_{III} -edge. The analysis of XANES spectra did not show significant modifications in intensity or energy of transitions as a function of temperature or PbTiO_3 content. Results obtained by the fitting of the EXAFS spectra revealed a local rhombohedral symmetry at 120 K for PFW composition, which is consistent with electrical properties of this compound. On the case of (PFW100xPT) multiferroic ceramics, for all studied compositions, the local structure around W atoms presents a local tetragonal symmetry with two short and four longer W-O bond-lengths well above the maximum of their dielectric temperature curve where a local cubic symmetry was expected.

5. Acknowledgements

Research partially carried out at LNLS National Laboratory of Synchrotron Light, Brazil. This study was supported by FAPESP and CNPq Brazilian financing agencies. The authors wish to thank Mr. Francisco J. Picon and Mrs. Natalia A. Zanardi for the technical assistance during sample preparation.

References

- [1] Cheong S-W and Mostovoy M 2007 *Nat. Mater.* **6** 13-20
- [2] Eiras J A, Fraygola B M and Garcia D 2010 *Key Eng. Mater.* **434-435** 307-10
- [3] Lu C H and Wong Y C 1995 *Ceram. Int.* **21** 413-9
- [4] Fraygola B M, Coelho A A, Garcia D and Eiras J A 2012 *Process. Appl. Ceramics* **6** 65-75
- [5] Michalowicz A, Moscovici, J., Muller-Bouvet, D., Provost, K. 2009 *J. Phys. Conf. Ser.* **190** 012034
- [6] Ankudinov A L, Ravel B, Conradson S D and Rehr J J 1998 *Phys. Rev. B* **58** 7565
- [7] Majewski P, Geprags S, Boger A, Opel M, Erb A, Gross R, Vaitheeswaran G, Kanchana V, Delin A, Wilhelm F, Rogalev A and Alff L 2005 *Phy. Rev. B* **72**
- [8] Mitoseriu L, Vilarinho P M, Viviani M and Baptista J L 2002 *Mater. Lett.* **57** 609-14
- [9] Ivanov S A, Eriksson S G, Tellgren R and Rundlof H 2004 *Mater. Res. Bull.* **39** 2317-28
- [10] Sicron N, Ravel B, Yacoby Y, Stern E A, Dogan F and Rehr J J 1994 *Phys. Rev. B* **50** 13168-80
- [11] Neves P P, Doriguetto A C, Mastelaro V R, Lopes L P, Mascarenhas Y P, Michalowicz A and Eiras J A 2004 *J. Phys. Chem. B* **108** 14840-9